Metallomics

PAPER

View Article Online
View Journal | View Issue



Cite this: *Metallomics*, 2014, 6, 2213

# Hg(II) bacterial biouptake: the role of anthropogenic and biogenic ligands present in solution and spectroscopic evidence of ligand exchange reactions at the cell surface†

Sara Anne Thomas, Tiezheng Tong and Jean-François Gaillard*

Received 27th June 2014,
Accepted 8th October 2014

DOI: 10.1039/c4mt00172a

www.rsc.org/metallomics

We have used a whole cell biosensor to investigate how the chemical speciation of aqueous Hg(II) affects its biouptake. The reporter system consists of a model gram-negative bacterium (*Escherichia coli*) with a chromosomally inserted *merR::luxCDABE* fusion. Synthetic aminopolycarboxylate organic ligands (EDTA, DTPA, EDDS, and NTA) as well as naturally-occurring thiol-containing ligands (cysteine, penicillamine, and glutathione) were used to control Hg(II) speciation in solution. We observed that all aminopolycarboxylate ligands promote the biouptake of Hg(II), following trends unexplained by Hg(II) speciation. Hg(II) biouptake was greatly enhanced in the presence of cysteine whereas it was inhibited in the presence of penicillamine and glutathione. Bioreporter exposure to increasing concentrations of Hg(II) quantitatively complexed by EDTA, DTPA, EDDS and cysteine showed that the extent of uptake is dose-dependent until a plateau is reached. Additionally, Hg $L_{III}$-edge X-ray absorption near edge structure (XANES) spectra of Hg(II) associated with the bioreporter membrane under the conditions used to perform the biouptake experiments suggest that a ligand exchange reaction occurs between the Hg(II)–aminopolycarboxylate complex and thiol moieties at the cell membrane. We conclude that ligand-exchange reactions at the cell surface play a critical role in the bacterial biouptake of Hg(II).

## Introduction

Understanding how chemical speciation influences the biouptake of metals is crucial to predict their fate in aquatic environments and the effect they have on living organisms. The ability of a metal to bind to a transport site located on a biological membrane plays a critical role in the biouptake process.[1] As a result, free metal ions and metals complexed with weak ligands are generally considered bioavailable, while trace metals complexed with high-affinity ligands are deemed non-bioavailable. The first model developed to predict trace metal bioavailability – the Free Ion Activity Model (FIAM) – states that the extent of uptake is proportional to the free ion metal concentration, which holds true in many cases.[2] However, many exceptions to the FIAM have also been observed.[2] This led to the development of a more comprehensive model – the biotic ligand model (BLM). The BLM incorporates important factors involved in trace metal biouptake overlooked by the FIAM including competitive ligand exchange reactions at biological interfaces as well as water quality parameters.[3]

Synthetic aminopolycarboxylate ligands (*e.g.*, EDTA, DTPA, EDDS and NTA) are excellent metal sequestering agents due to their stability and high affinities for metals. They are widely used in commercial and industrial applications and some are notorious for evading biodegradation during wastewater treatment.[4] In particular, EDTA is used in the textile industry, pulp and paper production, food products, cosmetics, and medicine; as a result, it has been detected in fresh surface waters at concentrations as high as 1120 μg $L^{-1}$.[5] Due to their distinctive properties, aminopolycarboxylate ligands are commonly used to control metal speciation in biouptake studies. These ligands have been shown to limit zinc biouptake by phytoplankton,[6] copper biouptake by phytoplankton,[7] and zinc and cadmium biouptake by two strains of cyanobacteria[8] among other examples.

Mercury (Hg) is considered one of the most hazardous contaminants present in aquatic environments, and it has caused the most fresh water fish advisories in the U.S. out of any other anthropogenically-released pollutant.[9] Hg inputs to surface waters can lead to the production of monomethylmercury(II) ($CH_3Hg^+$ or MeHg) – a potent neurotoxin that biomagnifies up trophic levels of aquatic food webs.[10] Certain

*Department of Civil and Environmental Engineering, Northwestern University, 2145 Sheridan Road, Evanston, IL, 60208, USA.*
*E-mail: jf-gaillard@northwestern.edu; Tel: +1-(847)-467-1376*

† Electronic supplementary information (ESI) available. See DOI: 10.1039/c4mt00172a

gram-negative anaerobic bacteria including sulfate-reducers and iron-reducers are primarily responsible for converting Hg(II) into MeHg,[11] and it is well accepted that the bacterial cell must internalize Hg(II) prior to methylation.[12] Thus, bacterial Hg(II) biouptake directly links environmental Hg inputs to human Hg exposure.

Little is known of the factors that regulate Hg(II) biouptake by bacteria, partially due to the difficulty of differentiating intracellular Hg(II) from Hg(II) adsorbed to the cell surface. Studies in the past have suggested passive diffusion of small, neutral Hg(II) complexes (*i.e.*, HgS and $HgCl_2$) as the pathway for bacterial Hg(II) biouptake.[13] In these studies, Hg(II) biouptake was found to correlate with the concentration of the neutral Hg(II) complex but not with the concentration of charged Hg(II) complexes (*e.g.*, $HgCl_3^-$) or the Hg(II) free ion. However, a recent study by Schaefer *et al.* discovered two species of Hg(II)-methylating bacteria internalize Hg(II) by active transport.[14] Because Hg(II) has no known biological function, Hg(II) taken up by active transport is likely adventitiously internalized by a transport protein. Additionally, many unanticipated findings regarding the relationship between Hg(II) speciation and bioavailability to bacteria have recently been reported in the literature including the biouptake of Hg(II) in the presence of excess EDTA,[15] the methylation of nanoparticulate Hg,[16] and high uptake and methylation rates of Hg(II) complexed with thiol-containing organic ligands.[14,17] It has been proposed that Hg(II) complexed with biogenic organic ligands (*i.e.*, cysteine and histidine) may be inadvertently internalized as a Hg(II) complex either by ligand transporters or metal transporters that evolved to internalize essential metals complexed with biogenic ligands.[1,14,17a,18] As Hg(II) speciation seems to control Hg(II) biouptake in ways different than previously thought, this topic must be explored further.

In this study, a genetically modified model gram-negative bacterium (*Escherichia coli*) was used to directly probe Hg(II) biouptake in the presence of high Hg(II)-affinity synthetic aminopolycarboxylate ligands (EDTA, DTPA, EDDS, and NTA) as well as naturally-occurring thiol-containing ligands (cysteine, penicillamine, and glutathione). This strain of *Escherichia coli* (*E. coli* ARL1) contains a chromosomally inserted *merR::luxCDABE* fusion and emits light at intensities proportional to the concentration of intracellular Hg(II). A biosensor method offers several advantages over other techniques to study Hg(II) biouptake including high-throughput capabilities and high reproducibility. Through controlled laboratory studies, the aim of this work was to compare the influence of two diverse groups of organic ligands on Hg(II) biouptake in hopes of gaining insight into underlying Hg(II) biouptake processes. We also used Hg $L_{III}$-edge X-ray absorption spectroscopy to assess the local binding environment of Hg(II) associated with the bioreporter cell membrane.

## Materials and methods

### Mercury biosensor – *Escherichia coli* ARL1

The bacterial strain *Escherichia coli* (*E. coli*) ARL1 used in this study is described in detail by Dahl *et al.*[15] Briefly, this strain contains a chromosomally inserted *merR::luxCDABE* fusion gene as well as a kanamycin resistance gene and emits light at an intensity proportional to the concentration of bioavailable Hg(II) in the exposure medium. The bioluminescent response is detectable in the presence of Hg(II) concentrations as low as 10 nM total dissolved Hg(II) (THg) in the exposure medium. It is highly sensitive to Hg(II) and stable due to the location of the *mer-lux* construct on the chromosome.

### Growth of cultures and growth media constituents

A single colony was picked up from an LB agar plate (50 μg $mL^{-1}$ kanamycin), inoculated into LB broth with 50 μg $mL^{-1}$ kanamycin, and incubated at 37 °C until mid-exponential phase ($OD_{600}$ of 0.3–0.4). Subsequently, the cell suspension was washed once with a minimal salts media (MSM), and 100 μL of the cell suspension was inoculated into 50 mL fresh MSM and incubated for approximately 24 hours at 37 °C. Once early exponential growth phase was reached ($OD_{600}$ ~0.2) in MSM, the cells were washed twice in a minimally complexing media (MCM) and resuspended in an equivalent volume of MCM. An $OD_{600}$ of 0.2 corresponds to a cell density of approximately $3 \times 10^8$ cells per mL. The MSM is used as a transient media to facilitate adjustment to nutrient-limited MCM – the exposure medium for the bioassays. The constituents of MCM were chosen to minimize compounds that complex Hg(II) and are reported with the constituents of MSM in Table S1 (ESI†).

### Bioreporter assays

A 1 mM $HgCl_2$ stock solution adjusted to pH 2 with trace metal grade HCl was used for the bioreporter assays. All Hg(II)–organic ligand solutions were prepared at 10 times the final desired concentration in Milli-Q water and pre-equilibrated for approximately 1 hour in polypropylene tubes. The bioluminescence assays were conducted in white polystyrene 96-well microtiter plates. Twenty microliters of pre-equilibrated Hg(II)–ligand solutions were added to assigned wells of the microplate, and the experiment was initiated with the addition of 180 μL of cell suspensions in MCM to each well so that the pre-equilibrated Hg solutions were diluted by a factor of 10. Each plate contained 3 replicates of all Hg samples, a blank (20 μL Milli-Q with 180 μL of cell suspension) as well as controls testing for the presence of Hg in the ligand stock solutions or growth media.

An FLx 800 Microplate reader (Biotek) was used to measure the luminescence intensity in each well every 5 minutes for exposure periods of 3 hours. A detector sensitivity of 200 was used for all measurements. Raw data were normalized to the blank by subtracting raw luminescence output (in relative luminescence units, RLU) by the raw luminescence output of the blank at each measurement time point. To confirm that light output is a viable indicator of the relative concentration of intracellular Hg(II), *E. coli* ARL1 was exposed to 0–100 nM THg in MCM in the absence of organic ligands.

To study Hg(II) biouptake, *E. coli* ARL1 was exposed to 30 nM THg in the presence of varying organic ligand concentration (0.1–1000 μM). To monitor the loss of Hg(II) due to adsorption onto the walls of the well plate in the presence of varying

 

organic ligand concentrations, THg in the wells was measured with a Direct Mercury Analyzer (DMA-80, Milestone) after the 3 hour exposure period. In addition, the biosensor was exposed to a constant organic ligand concentration of 1 mM in the presence of varying THg concentrations (25–500 nM Hg with EDTA, DTPA, and EDDS and 10–500 nM Hg with cysteine) for 3 hours.

The growth of *E. coli* ARL1 in MCM under the same conditions as biouptake experiments was assessed to determine if the experimental conditions had a major influence on cell physiology. Growth tests were conducted over a 7 hour time period in clear bottom 96-well polystyrene plates, and plates were shaken gently at 25 °C in the dark. The $OD_{600}$ was measured every hour of the exposure period by an ELx800 Microplate Reader (Biotek). The initial $OD_{600}$ of *E. coli* ARL1 in MCM was approximately 0.18 for all growth tests.

### XAS sample preparation, measurements, and data analysis

Samples analyzed by X-ray absorption spectroscopy (XAS) were prepared in the same way as the bioreporter assays with a few minor adjustments: *E. coli* ARL1 was grown to late-exponential growth phase in MSM ($OD_{600}$ ~0.3) and diluted to a final $OD_{600}$ of 0.2 in MCM, the glucose was eliminated from the MCM recipe, and 90 mL cell suspension in MCM (no glucose; final $OD_{600}$ = 0.2) was exposed to 10 mL Hg(II)–ligand solution in Erlenmeyer flasks. The samples included cells exposed to 500 nM Hg and 50 μM Hg pre-equilibrated with 1 mM EDTA as well as 500 nM Hg and 50 μM Hg in the absence of chelating organic ligand. After the addition of cell suspensions to Hg solutions, the flasks were shaken gently for 3 hours in the dark at 25 °C. Cell suspensions were then washed 3 times by centrifugation with 0.1 M $NaClO_4$ to remove the remaining Hg in solution. The supernatant was discarded after the last wash, the remaining cell pellet was spread onto filter paper (0.2 μm), and excess moisture was removed with a vacuum pump. Residual biomass on the filter paper was sandwiched between 2 pieces of Kapton tape and refrigerated until analysis the next day.

Hg $L_{III}$-edge XANES spectra were collected at the DuPont-Northwestern-Dow Collaborative Access Team (DND-CAT) beamline located in Sector 5 of the Advanced Photon Source at Argonne National Laboratory. A detailed description of techniques used to prepare Hg reference standards and collect and analyze the data is provided in the ESI.†

### Cell-sorption and intracellular Hg(II) experiments

To determine the fraction of Hg(II) in the cytoplasm as well as bound to the cell surface of samples prepared for XAS measurements, the sorbed and intracellular Hg(II) concentration was determined for cells exposed to 500 nM Hg(II) in the presence and absence of 1 mM EDTA for 3 hours in MCM without glucose as well as MCM with glucose for comparison. Sorbed Hg(II) was also determined for cells suspended in MCM without glucose exposed to 50 μM Hg(II) in the presence and absence of 1 mM EDTA.

When MCM with glucose or MCM without glucose was used as the exposure medium, cells were grown according to the method used in biouptake experiments or XAS experiments, respectively. The experiment began with the addition of 4.5 mL cell suspension in MCM with or without glucose to 0.5 mL of pre-equilibrated Hg(II)–organic ligand solution in 15 mL glass vials. Sorbed Hg(II) was calculated as the total concentration of Hg(II) in suspension subtracted by the dissolved concentration of Hg(II) (passed through 0.2 μm nylon filter; VWR International). Intracellular Hg(II) concentration was calculated as the total concentration of Hg(II) in suspension subtracted by the concentration of Hg(II) in the filtrate after a cell-wash procedure designed to remove all Hg(II) bound to the cell membrane.[14] The wash was performed by filtering 4 mL of cell suspension through a 0.2 μm nylon filter followed by 10 mL of 50 mM EDTA, 100 mM oxalate, 10 mM KCl solution, 20 mL of 3 mM glutathione, 1 mM ascorbate solution, and 5 mL of MCM solution without glucose. The filtrate from the wash was collected and analyzed for total Hg(II) immediately after sample collection with a Direct Mercury Analyzer (DMA-80, Milestone).

### Calculation of Hg speciation

The Hg speciation in the exposure medium as well as in the pre-equilibrated Hg(II)–organic ligand solutions was calculated with ChemEQL[19] for each exposure condition. The reactions between Hg(II) and MCM components were considered in speciation calculations with the exception of glucose, MOPS buffer, β-glycerophosphate, and thiamine, since, to our knowledge, no thermodynamic constants have ever been reported. The complexation constants for Hg(II) and the chelating organic ligands used in this study are included in Table S1 (ESI†). All equilibrium constants were obtained from the Joint Expert Speciation System (JESS) database[20] or otherwise cited.

### Chemical reagents

The $HgCl_2$, $HgNO_3$, and all organic ligands used in this study were obtained from Sigma-Aldrich. The thiol-containing ligands were used within 1 year of purchase date.

## Results

### Bioluminescent response proxy for bioavailable Hg(II) in exposure medium

The applicability of using luminescence output by *E. coli* ARL1 as a proxy for studying Hg(II) biouptake was confirmed by recording the relative luminescence intensity in the presence of 0–100 nM THg in MCM every 5 minutes for 3 hours. Hg(II) speciation in MCM (pH = 7.1) in the absence of chelating organic ligands is dominated by $Hg(isoleucine)_2$ and $Hg(NH_3)_2^{2+}$. A sigmoidal time–response curve was observed (Fig. S1, ESI†), which is common among other biosensors with a *mer-lux* construct.[13b,15,18] The maximum luminescence signal for each Hg concentration recorded during the 3 hour exposure was plotted against THg, yielding a linear relationship with a 5.0% uncertainty (±1 SD) on the slope of the regression (Fig. 1). Maximum luminescence signal increases with THg up to 300 nM THg, above which the signal decreases with increasing

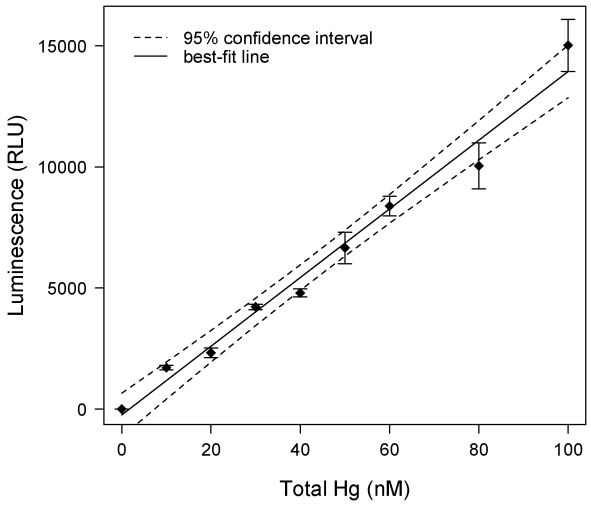


Fig. 1 The maximum luminescence reported in relative luminescence units (RLU) detected over a 3 hour exposure period of *E. coli* ARL1 to 0–100 nM THg in MCM plotted against THg. Under these conditions, Hg(II) speciation in MCM (pH = 7.1) is dominated by $Hg(isoleucine)_2$ and $Hg(NH_3)_2^{2+}$. The points represent the average of 3 replicates, and error bars are ±1 SD.

THg (data not shown). Growth curves of *E. coli* ARL1 in MCM with 0–500 nM THg for a 7 hour exposure period illustrate dose-dependent growth inhibition beginning at 200 nM THg (Fig. S2, ESI†). This suggests that Hg(II) might affect cellular metabolism and hence impact the bioluminescent response at concentrations above 200 nM THg. Growth inhibition after 3 hours was not as noticeable as after 7 hours, thus a 7 hour exposure period was used for all growth studies.

### Facilitated Hg(II) biouptake observed in presence of biogenic and synthetic organic ligands

To determine the influence of organic ligand concentration on the uptake of Hg(II), luminescence emitted by *E. coli* ARL1 in the presence of 30 nM THg pre-equilibrated with 0.1–1000 μM aminopolycarboxylate and thiol-containing ligands was recorded at 5 minute intervals over a 3 hour exposure period. A sigmoidal time–response curve was observed in the presence of all concentrations of all organic ligands except for 100 and 1000 μM cysteine, where luminescence signal did not fully plateau during the exposure time. To compare relative Hg(II) biouptake efficiency in the presence of different ligands, the results were normalized by dividing the maximum luminescence signal of each sample by the maximum signal of a 30 nM THg control with no organic ligand from the same experiment (Fig. 2). The speciation of Hg(II) for each exposure condition is presented in Table 1. Additionally, the speciation of Hg(II) in the pre-equilibrated Hg(II)–organic ligand solutions is provided in Table S3 (ESI†). The strength of the complexing ligand, from strongest to weakest, is DTPA > EDTA > EDDS > NTA for the aminopolycarboxylate ligands and glutathione > penicillamine > cysteine for the thiol-containing ligands (Table S1, ESI†).

The luminescence output in the presence of all aminopolycarboxylate ligands at concentrations between 0.1–100 μM was either enhanced or unchanged compared to the control, even though speciation calculations predict that Hg(II) is 100% bound to DTPA above 0.1 μM DTPA and more than 99.9% bound to EDTA at 100 μM EDTA in MCM. When the concentration of aminopolycarboxylate ligand equals 1000 μM, speciation calculations indicate Hg(II) is 100% complexed with EDTA and DTPA

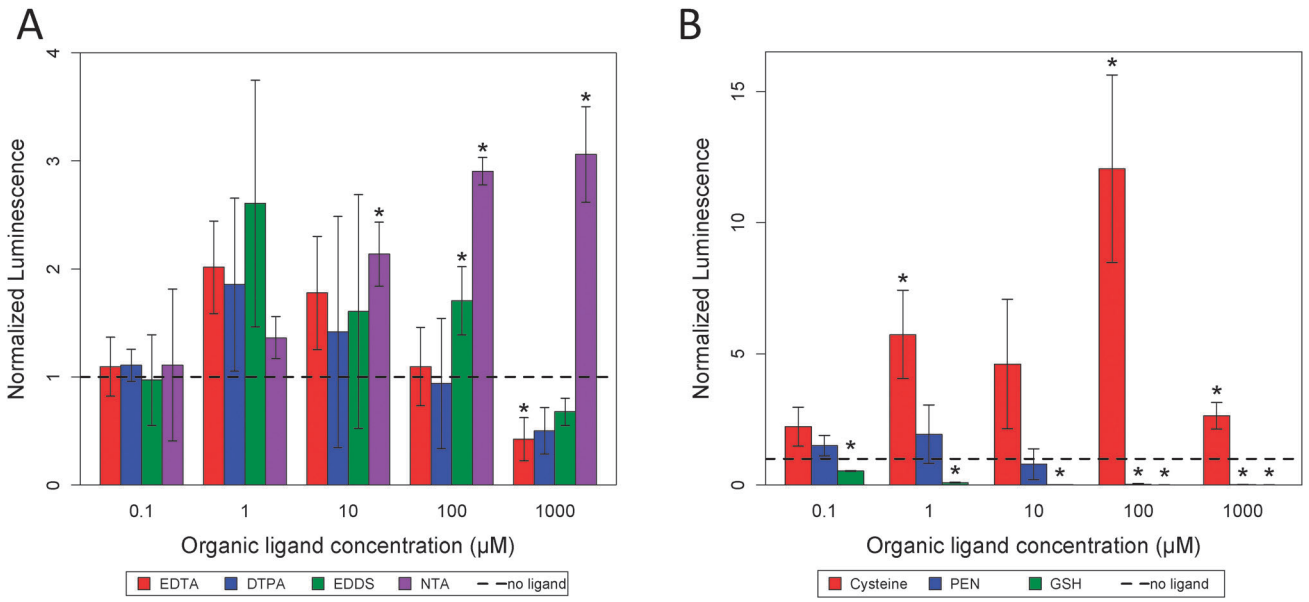


Fig. 2 Normalized luminescence recorded for a 3 hour exposure period of *E. coli* ARL1 to 30 nM THg in the presence of various concentrations of (A) aminopolycarboxylate ligands and (B) thiol-containing ligands in MCM (pH = 7.1). The luminescence of each sample was normalized to a 30 nM THg control with no organic ligand by dividing the maximum signal of the sample by the maximum signal of the control that was recorded during the exposure period. Hg was pre-equilibrated with the organic ligand in Milli-Q water for 1 hour prior to cell exposure. The bars represent averages of 2 to 4 independent experiments (typically $n$ = 3), error bars are ±1 SD, and the asterisk symbolizes data statistically different from the control ($p < 0.05$).

 

Table 1 Speciation (as % THg) of 30 nM THg in the presence of different concentrations of organic ligands in MCM (pH = 7.1)[a]

| Organic ligand (μM) | | 0.1 | 1 | 10 | 100 | 1000 |
|---|---|---|---|---|---|---|
| EDTA | $HgEDTA^{2-}$ | 46.4 | 90.6 | 98.8 | 99.7 | 99.73 |
| | $HgOHEDTA^{3-}$ | 0.10 | 0.19 | 0.21 | 0.21 | 0.25 |
| | $HgHEDTA^{-}$ | 0.01 | 0.02 | 0.02 | 0.02 | 0.02 |
| NTA | $HgNTA^{-}$ | 0.012 | 0.12 | 1.18 | 11.1 | 61.06 |
| EDDS | $HgEDDS^{2-}$ | 1.16 | 8.78 | 25.45 | 31.40 | 31.50 |
| | $HgOHEDDS^{3-}$ | 2.43 | 18.41 | 53.45 | 65.90 | 68.14 |
| | $HgHEDDS^{-}$ | — | 0.04 | 0.12 | 0.15 | 0.15 |
| DTPA | $HgDTPA^{3-}$ | 99.81 | 99.90 | 99.91 | 99.90 | 99.88 |
| | $HgHDTPA^{2-}$ | 0.09 | 0.09 | 0.09 | 0.10 | 0.12 |
| Cysteine | $Hg(Cys)_2^{2-}$ | 0.53 | 0.53 | 0.53 | 0.56 | 0.54 |
| | $HgH(Cys)_2^{-}$ | 35.43 | 35.43 | 35.51 | 36.27 | 35.31 |
| | $HgH_2(Cys)_2$ | 64.04 | 64.04 | 63.94 | 62.92 | 61.84 |
| | $HgH(Cys)_3^{3-}$ | — | — | — | 0.02 | 0.06 |
| | $HgH_2(Cys)_3^{2-}$ | — | — | 0.02 | 0.23 | 2.25 |
| Penicillamine (PEN) | $HgH_2(PEN)_2$ | 100 | 99.99 | 99.91 | 99.09 | 91.73 |
| | $HgH_3(PEN)_3^{-}$ | — | 0.01 | 0.09 | 0.91 | 8.27 |
| Glutathione (GSH) | $HgH(GSH)_2^{3-}$ | 1.25 | 1.25 | 1.25 | 1.22 | 0.98 |
| | $HgH_2(GSH)_2^{2-}$ | 98.75 | 98.75 | 98.72 | 98.45 | 96.37 |
| | $HgH_2(GSH)_3^{3-}$ | — | — | — | 0.01 | 0.04 |
| | $HgH_3(GSH)_3^{4-}$ | — | — | 0.03 | 0.32 | 2.61 |

[a] Some percentages do not add up to 100 as only Hg(II)-organic ligand species are included.

and 99.8% complexed with EDDS in MCM and luminescence output is approximately 42%, 50%, and 68% of the control respectively. On the other hand, the presence of 1000 μM NTA enhanced the bioluminescence signal by a factor of 3. One should note, however, that NTA forms the weakest Hg(II) complex of the aminopolycarboxylates. Speciation calculations show that Hg(II) is only 61% complexed with NTA in the presence of 1000 μM NTA, where the other dominant Hg(II) species are $Hg(isoleucine)_2$ and $Hg(NH_3)_2^{2+}$.

The growth of *E. coli* ARL1 during a 3 hour exposure period was not affected by the presence of aminopolycarboxylate ligands, whereas over a 7 hour period concentrations of 0.1–1000 μM EDTA and DTPA, 1–1000 μM EDDS, and 100–1000 μM NTA induced a noticeable decrease in cell density compared to the control. This suggests that aminopolycarboxylates may produce a chronic toxicity effect that influences cell physiology (Fig. S3, ESI†). However, this effect on cell physiology does not explain the observed enhanced or unchanged biouptake results but may be responsible for reducing luminescence output. Additionally, the loss of Hg(II) due to well plate adsorption was measured after the 3 hour exposure period, and recoverable Hg(II) in the presence of 0.1–1000 μM EDTA, DTPA, EDDS, and NTA was not significantly different than the control with no organic ligand (Fig. S4, ESI†).

The presence of cysteine facilitates Hg(II) biouptake, the extent of which appears to increase with cysteine concentration until 100 μM cysteine yields a 12-fold increase over the control. The presence of 1000 μM cysteine only yields a 3-fold increase. This trend correlates well with Hg methylation rates that were observed for the iron reducer *Geobacter sulfurreducens* in the presence of similar ratios of Hg(II) to cysteine.[17a] In contrast, lower concentrations of penicillamine slightly facilitated Hg(II) uptake, and the presence of 100 and 1000 μM penicillamine and 10–1000 μM glutathione inhibited Hg(II) uptake. With a plasmid-based mer-lux bioreporter, Ndu *et al.* observed enhanced Hg(II) biouptake in the presence of cysteine and inhibited Hg(II) biouptake in the presence of glutathione as well.[17b]

The presence of all concentrations of penicillamine and glutathione and 0.1–100 μM cysteine had minor influence on cell growth in MCM for a 3 hour and 7 hour exposure period (Fig. S3, ESI†). A cysteine concentration of 1000 μM slightly inhibited growth compared to the control for 3- and 7 hour exposure periods, most likely due to bactericidal effects of cysteine exposed to molecular oxygen.[21] The loss of Hg(II) because of adsorption to well-plate walls in the presence of thiols was similar to the control for 0.1–10 μM cysteine and GSH as well as 0.1 μM PEN (Fig. S4, ESI†). The presence of 10 μM PEN limited adsorption by approximately a factor of 1.5 and 1000 μM cysteine, PEN, and GSH limited adsorption by nearly a factor of 2. Thus, enhanced Hg(II) bioavailability in the presence of 1000 μM cysteine compared to the control could be influenced by a greater dissolved Hg(II) concentration throughout the duration of the uptake experiment. As molecular oxygen is a substrate in the bioluminescence reaction,[22] the consumption of oxygen by 1000 μM penicillamine and glutathione was assessed in a solution of MCM sealed from the atmosphere for 3 hours (Fig. S5, ESI†). Neither ligand consumed enough oxygen to inhibit bioluminescence at those ligand concentrations.

### Uptake of Hg(II)–ligand complexes saturates with increasing complex concentration

The influence of Hg(II)–organic ligand complex concentration on Hg(II) biouptake was explored further by exposing the biosensor cells to 0–500 nM Hg(II) 100% complexed with EDTA, DTPA, EDDS and cysteine (constant ligand concentration of 1 mM) for 3 hour exposure periods. Only Hg(II) complexes with the above ligands are included because Hg(II) uptake is observed when Hg(II) is 100% complexed with the ligand in MCM and during pre-equilibration in Milli-Q. For each concentration of Hg(II)–organic ligand complex analyzed, the maximum luminescence signal recorded during the exposure period was plotted against the complex concentration, which is equivalent to THg in this case (Fig. 3). A sigmoidal dose–response curve was observed for all Hg(II)–aminopolycarboxylate complexes as well as the Hg(II)–cysteine complex. The dose–response curve for Hg(II) in the absence of organic ligand is included in Fig. 3 for comparison.

Dose–response curves are markedly different when Hg(II) is 100% complexed with organic ligands compared to Hg(II) in the absence of organic ligands. Most notably, the maximum luminescence output plateaus with increasing THg in the presence of organic ligands and peaks in their absence. For the concentrations tested, maximum luminescence is stable between 100–500 nM Hg(II)–cysteine, 150–500 nM Hg(II)–EDDS, 300–500 nM Hg(II)–EDTA, and 300–500 nM Hg(II)–DTPA. As we previously attributed

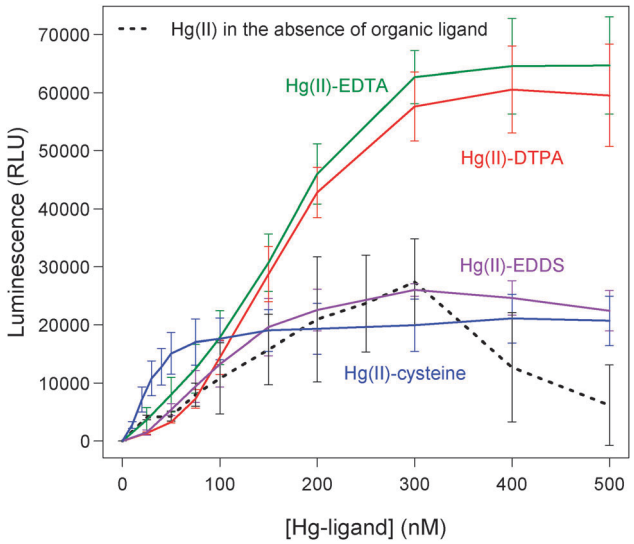


Fig. 3 The maximum luminescence intensity reported in relative luminescence units (RLU) recorded over a 3 hour exposure period of *E. coli* ARL1 to various concentrations of Hg(II) 100% complexed with EDTA, DTPA, EDDS, and cysteine. The dose–response curve for Hg(II) in the absence of organic ligand is included for comparison (dashed line). Hg(II) complexes were pre-equilibrated for 1 hour in Milli-Q water (different concentrations of $HgCl_2$ with 10 mM organic ligand) prior to cell exposure in MCM (pH = 7.1). The points represent the average of 3 independent experiments, and error bars are ±1 SD.

the drop in luminescence intensity above 300 nM THg in the absence of organic ligand to Hg toxicity and not decreased Hg bioavailability, the presence of organic ligands seems to prevent this effect. For organisms containing the complete *luxCDABE* gene cassette, the fatty aldehyde substrate required for bioluminescence is produced and recycled by the organism and is thus often the rate limiting substrate.[22,23] The addition of 400 ppm (v/v) aldehyde (decanal), which can be used to saturate the luminescent response, to assays with 25–500 nM Hg(II)–EDTA and Hg(II)–cysteine had no effect on luminescence (data not shown). Therefore, we conclude that the luminescence plateau observed for increasing Hg(II)–organic ligand complex concentrations is due to the saturation of intracellular Hg (*i.e.*, the uptake mechanism) and not to rate limiting substrates in the luminescence reaction.

From Fig. 3, it is apparent that lower concentrations of Hg(II) complexed with cysteine have higher biouptake efficiencies compared to the same concentrations of Hg(II) complexed with the aminopolycarboxylate ligands or in the absence of organic ligand. In addition, it is notable that the plateau in luminescence occurred at much higher luminescence intensities for Hg(II) complexed with EDTA and DTPA compared to EDDS and cysteine, indicating high Hg(II) concentrations are more bioavailable in the presence of EDTA and DTPA within a 3 hour exposure period.

### XANES spectra reveal ligand exchange between Hg(II)–EDTA complex and membrane bound thiols

To gain insight into the binding environment of Hg(II) associated with the cell membrane under the conditions used during the Hg(II) biouptake experiments, Hg $L_{III}$-edge XAS spectra were collected for a selection of samples of Hg(II) adsorbed to *E. coli* ARL1, as well as Hg reference standards (Fig. 4A). To limit active Hg(II) internalization by *E. coli* ARL1, glucose was eliminated from the exposure medium (MCM) used for sample preparation. Sample conditions of *E. coli* ARL1 exposed to 500 nM THg with no chelating organic ligand as well as 500 nM THg pre-equilibrated with 1 mM EDTA were chosen to determine if a ligand–exchange reaction occurs between Hg(II)–EDTA and the cell membrane at Hg(II) concentrations used during biouptake experiments. Samples of *E. coli* ARL1 exposed to a higher THg concentration (50 μM Hg) in the absence and presence of 1 mM EDTA were analyzed for comparison. Speciation calculations indicate that 500 nM and 50 μM Hg are 100% complexed with EDTA for the above exposure conditions and in pre-equilibrated Hg(II)–organic ligand solutions. Due to the number of scans required to obtain spectra of sufficient quality and a time restraint, EDTA was the only aminopolycarboxylate ligand examined.

Due to the very low concentration levels of Hg(II) in the bacterial samples analyzed, only the XANES spectra are presented, which document how the average local environment of Hg changes. The XANES spectra of cells exposed to 500 nM Hg(II) with no organic ligand, 500 nM Hg(II) with 1 mM EDTA, and 50 μM Hg(II) with 1 mM EDTA are nearly identical (Fig. 4B); noise contributes to the slight spectral differences. Therefore, we conclude that the predominant binding environments of Hg(II) sorbed to the cell surface initially exposed to cells as 500 nM Hg(II) with no organic ligand, 500 nM Hg(II) with 1 mM EDTA, and 50 μM Hg(II) with 1 mM EDTA are similar. Consequently, Hg(II) must dissociate from EDTA and bind to a biotic ligand located at the cell surface (*i.e.*, a ligand exchange occurs). The spectra of the Hg–EDTA standard is superimposed on the spectra of Hg-cell samples in Fig. 4B to show that no significant amount of Hg(II) remains complexed with EDTA while bound to the cell membrane. As aminopolycarboxylate ligands are characterized by similar functional groups, we infer that Hg(II) complexed with the other aminopolycarboxylate ligands is likely to undergo a similar ligand exchange at the cell membrane. Additionally, the XANES spectrum of cells exposed to 500 nM Hg(II) with no EDTA (and hence 500 nM and 50 μM Hg with 1 mM EDTA) appears to be a combination of the spectra of the $Hg(cysteine)_2$ and $Hg(cysteine)_3$ standards (Fig. 4C). This suggests Hg(II) is bound to between 2 and 3 thiol moieties at the cell membrane (likely cysteine residues of membrane proteins).

In Fig. 4B, we show that 1 mM EDTA influences the binding of 50 μM Hg(II) to the cell membrane as the spectra of 50 μM Hg(II) in the presence and absence of EDTA are notably different. In particular, the spectrum of 50 μM Hg(II) sorbed to the cells in the absence of EDTA has a sharp pre-edge peak at 12 285 eV that resembles the sharp pre-edge peak of $Hg(acetate)_2$ at the same energy (Fig. 4A). This is an indication that EDTA limits the binding of Hg(II) to the carboxyl groups also present at gram-negative cell membranes.[24] The finding that Hg(II) will preferentially bind to thiol groups and then more abundant oxygen/nitrogen-containing groups with increasing Hg(II) concentration has been reported for other microorganisms[25] as well as NOM.[26]

 

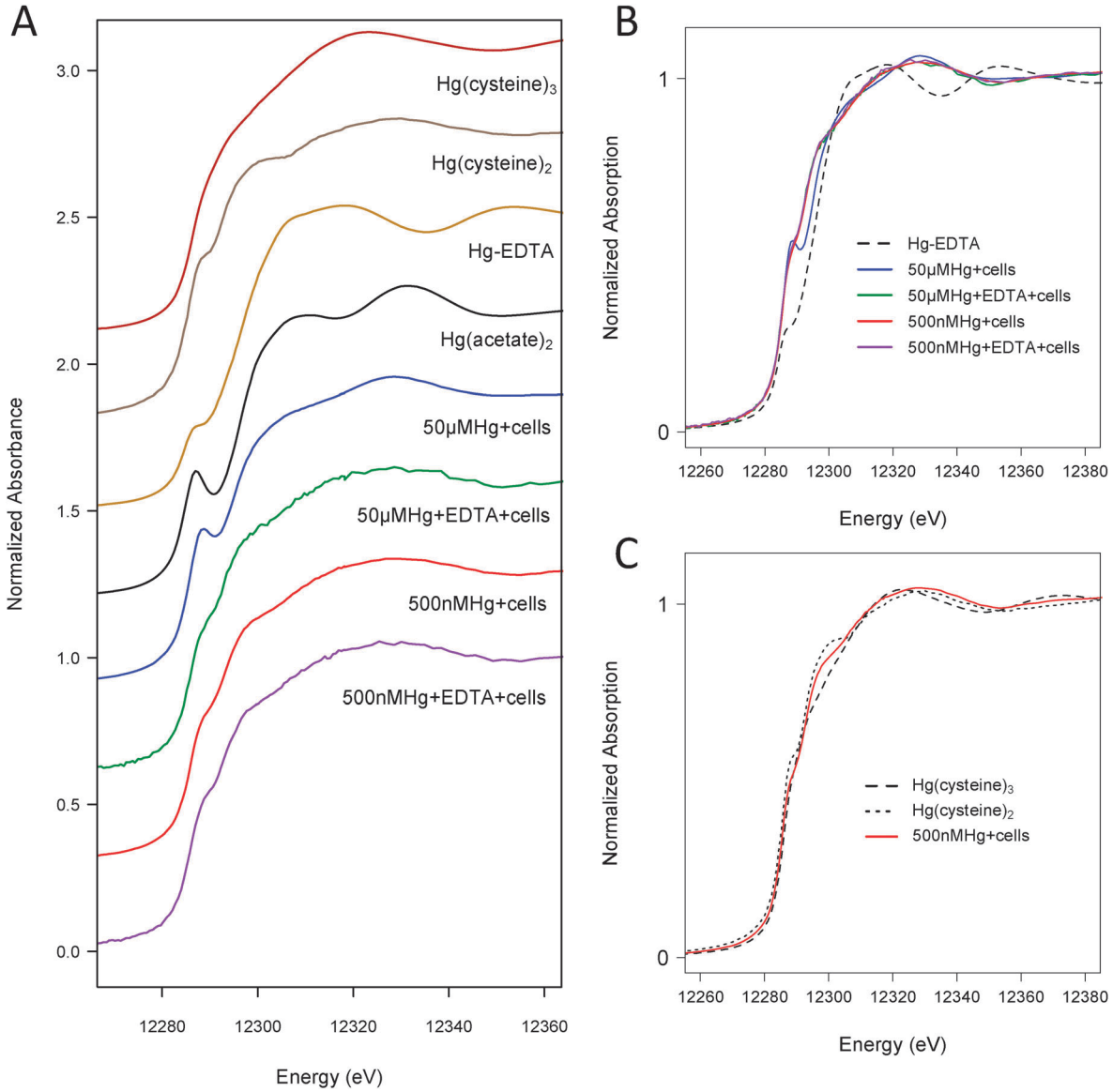


Fig. 4 Hg $L_{III}$-edge XANES spectra of Hg(II) sorbed to *E. coli* ARL1 initially introduced to bacterial cells as 50 μM and 500 nM Hg pre-equilibrated with 1 mM EDTA (500 nM, 50 μM Hg + EDTA + cells) or in the absence of organic ligand (500 nM, 50 μM Hg + cells). The exposure medium was MCM with no glucose (pH = 7.1) and cell density was approximately $3 \times 10^8$ cells per mL. (A) Normalized Hg $L_{III}$-edge XANES spectra of Hg samples plotted with Hg standards for qualitative comparison. (B) Normalized Hg $L_{III}$-edge XANES spectra of superimposed Hg samples (500 nM, 50 μM Hg ±1 mM EDTA exposed to cells) and the Hg–EDTA standard. The spectra of 500 nM Hg + cells, 500 nM Hg + EDTA + cells and 50 μM Hg + EDTA + cells overlap and are nearly indistinguishable. (C) Normalized Hg $L_{III}$-edge XANES spectra of Hg bound to the cell membrane initially exposed to cells as 500 nM Hg, the $Hg(cysteine)_2$ standard, and the $Hg(cysteine)_3$ standard.

### Cell sorption and wash experiments confirm Hg(II) undergoes ligand exchange with cell membrane and show Hg(II) uptake is energy-dependent

To verify that Hg(II) is only present at the cell membrane and not in the cytoplasm of cells prepared for XAS measurements, the overall concentration of Hg(II) associated with cells (sorbed Hg(II)) and the concentration of Hg(II) in the cytoplasm (intracellular Hg(II)) were measured for cells exposed to 500 nM Hg(II) in the presence and absence of 1 mM EDTA (Fig. 5). The exposure medium used was MCM with no glucose (same for XAS measurements) as well as MCM containing glucose (same for biouptake measurements). In MCM with glucose, approximately 94% and 98% of the total Hg(II) was sorbed to cells in the presence of 500 nM Hg(II) and 500 nM Hg(II) with 1 mM EDTA, respectively. However in MCM without glucose, about 44% and 24% of the total Hg(II) was sorbed to cells in the presence of 500 nM Hg(II) and 500 nM Hg(II) with 1 mM EDTA, respectively. Similar to results reported in Schaefer *et al.*,[14] no intracellular Hg(II) was detected when an exposure medium without a carbon source was used (MCM with no glucose). The addition of glucose to MCM enabled around 54% and 70% of the total Hg(II) to be internalized into the cytoplasm for 500 nM Hg(II) and 500 nM Hg(II) with 1 mM EDTA, respectively.

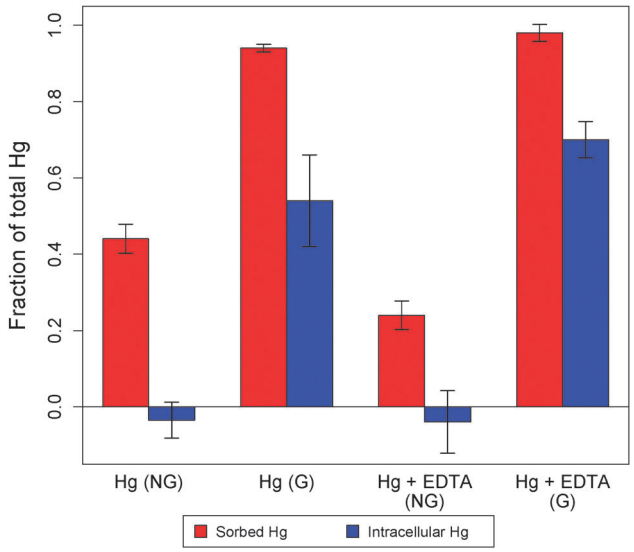


Fig. 5 The fraction of THg associated with (sorbed Hg) as well as solely in the cytoplasm of (intracellular Hg) *E. coli* ARL1 after a 3 hour exposure period to Hg as 500 nM Hg in the absence of organic ligand (Hg (NG), Hg (G)) or in the presence of 1 mM EDTA (Hg + EDTA (NG), Hg + EDTA (G)). The exposure medium was MCM with glucose (G) and MCM without glucose (NG) and cell density was approximately $3 \times 10^8$ cells per mL. The fraction of sorbed Hg was calculated as the concentration of dissolved Hg (passed through 0.2 μm filter) subtracted from THg then divided by THg. The fraction of intracellular Hg was calculated as the concentration of dissolved Hg (passed through 0.2 μm filter) after a washing procedure that removes Hg from cell membrane subtracted from THg then divided by THg. The bars represent averages from at least 3 independent experiments, and error bars are ±1 SD.

Sorption to cells in the presence of 50 μM Hg(II) and 50 μM Hg(II) with 1 mM EDTA in MCM without glucose was also determined (Fig. S6, ESI†). Around 60% of the total Hg(II) was sorbed in the absence of EDTA while the presence of 1 mM EDTA greatly limited Hg(II) sorption, explaining the differences in Hg(II)-cell binding environment observed with XAS for these conditions.

As intracellular Hg(II) is only detected when a carbon source is available, it indicates that Hg(II) biouptake is energy-dependent for this strain of *E. coli* (*i.e.*, uptake occurs by active transport). It is notable that Hg(II) sorption results are significantly different for 500 nM Hg(II) assays when the exposure medium includes and excludes glucose. We attribute this effect to the large fraction of THg that is internalized when glucose is present contributing to the sorbed fraction of Hg. In fact, the fraction of Hg(II) bound to the cell membrane is nearly identical in the presence and absence of glucose (40% and 28% with glucose *versus* 44% and 24% without glucose for 500 nM Hg(II) and 500 nM Hg(II) with 1 mM EDTA, respectively). Additionally, the finding that no intracellular Hg(II) was detected when MCM without glucose was used as the exposure medium supports that the ligand exchange observed by XAS occurs at the cell membrane.

## Discussion

As Hg(II) biouptake by *E. coli* ARL1 is an energy dependent process and it is unlikely that bulky, charged Hg(II)–organic ligand complexes passively diffuse through the cell membrane, we conclude that Hg(II) is internalized by a transport protein. Our finding that Hg(II) uptake saturates with an increasing concentration of the Hg(II)–organic ligand complex is consistent with uptake by a transport protein and not by passive diffusion as well. The only known Hg(II) transport proteins (MerT and MerC) are included in the Hg resistance-encoding *mer operon*,[27] which is absent in *E. coli* ARL1. Thus, Hg(II) uptake is presumably inadvertent. Hg(II) complexed with aminopolycarboxylate ligands in solution would likely be internalized by a metal transport protein, as there are no known aminopolycarboxylate transporters to our knowledge. Additionally, Schaefer *et al.* suggest that gram-negative bacteria internalize Hg(II)–cysteine complexes *via* a metal transporter and not an amino acid transporter because uptake is not affected by chirality.[14] Most metal transporters are located in the cytoplasmic membrane of gram-negative bacteria,[28] meaning Hg(II) would have to cross the outer membrane (OM) and traverse the periplasm prior to uptake.

The finding that a ligand-exchange reaction occurs between Hg(II)–EDTA and a biotic ligand at the cell membrane brings up the question of whether the ligand-exchange is actually involved in Hg(II) uptake. It is notable that Hg(II) biouptake was observed and even enhanced in the presence of all concentrations of aminopolycarboxylate ligands and cysteine, while concentrations of penicillamine and glutathione above 100 μM completely inhibited Hg(II) uptake. Nuclear magnetic resonance (NMR) data show that Hg(II) complexes with cysteine, penicillamine, and glutathione are all labile;[29] thus, the observed inhibition of Hg(II) uptake by penicillamine and glutathione is seemingly of a thermodynamic nature. Penicillamine and glutathione have the highest affinity for Hg(II) of the ligands in this study (Table S1, ESI†), suggesting the stabilities of the Hg–PEN and Hg–GSH complexes inhibit a ligand exchange reaction and hence Hg(II) biouptake. Since the XANES data show that the ligand exchange occurs with membrane thiols, differences in Hg(II) binding affinities among exogenous thiols can control metal uptake. We also observe that biouptake trends of Hg(II) 100% complexed with ligands of both synthetic (EDTA, DTPA, and EDDS) and biogenic (cysteine) origin are similar in that they all plateau after a certain Hg–organic ligand complex concentration. If the uptake of a Hg(II)–organic ligand complex depended on a ligand-exchange reaction with a specific metal transport protein, uptake in the presence of all chelating organic ligands able to exchange Hg(II) – regardless of origin – would be expected to be similar.

Our results indicate that the presence of certain organic ligands will affect Hg(II) biouptake in ways unpredictable by Hg(II) speciation or even total Hg(II) sorbed to cells, suggesting bacterial Hg(II) biouptake is a complicated process that is likely influenced by a combination of factors. For example, we observe that 1 mM EDTA limits the extra-cytoplasmic sorption of 500 nM THg but actually enhances the intracellular concentration of Hg(II). This result could be caused by a competition effect between the abundance of membrane proteins in the periplasm[30] and exogenous organic ligands, as Hg(II) is known to have high affinities for various amino acids.[31] A competition

 

with low-affinity periplasmic proteins not involved in Hg(II) uptake would increase the periplasmic mobility of Hg(II) and the probability that Hg(II) reaches the 'correct' high-affinity transport protein responsible for its internalization. Cell physiology must also play a role in Hg(II) biouptake, as it is well documented that cells will adjust the activity of their metal transport mechanisms under different environmental conditions.[28] For example, the presence of excess organic ligands may enhance Hg(II) biouptake simply because they sequester the pool of essential trace metals in the exposure medium and trigger increased metal transporter activity. A better understanding of cell physiology under the exposure conditions of this study may explain our observed Hg(II) uptake trends, especially those in the presence of varying concentrations of the aminopolycarboxylate ligands and cysteine.

## Conclusion

While the specific transport mechanism responsible for internalizing Hg(II) has yet to be discovered, this study demonstrates that (a) the facilitated biouptake of Hg(II) complexed with organic ligands is not limited to biogenic ligands but also occurs with synthetic ligands, (b) thiols at the cell membrane are able to outcompete aqueous complexing agents with high Hg(II) affinities and bind Hg(II) through a ligand-exchange reaction, and (c) Hg(II) uptake in *E. coli* is an energy-dependent process. We propose that Hg(II) is internalized adventitiously by an essential metal transporter and that a ligand exchange with a biotic ligand at the cell membrane determines the bioavailability of Hg(II)–organic ligand complexes.

The observation of facilitated Hg(II) biouptake and Hg(II) accumulation at the cell membrane when Hg(II) is 100% complexed with synthetic aminopolycarboxylate ligands contradicts the FIAM and suggests that the BLM may be a more appropriate model to assess Hg(II) bioavailability. In addition, the ability of thiols at the cell membrane to outcompete aqueous ligands with high Hg(II) affinities and bind Hg(II) has implications for Hg(II) fate and transport in the environment.

## Acknowledgements

We thank Amy Dahl, Luciana Zanella, and Isabelle (Xixi) Ji for their valuable insight regarding the experimental design as well as William Oestreich for his help conducting bioreporter assays. We also thank Qin Ma for his beamline assistance at the APS. Portions of this work were performed at the DND-CAT Synchrotron Research Centre located at Sector 5 of the APS. DND-CAT is supported by the E.I. DuPont de Nemours & Co., The Dow Chemical Company, the U.S. National Science Foundation through Grant DMR-9304725, and the State of Illinois through the Department of Commerce and the Board of Higher Education Grant IBHE HECA NWU 96. This work is supported by the National Science Foundation under grant CHE-1308504 and an undergraduate and graduate student research grant from the Initiative for Sustainability and Energy (ISEN) at Northwestern University to S.A.T. and T. T., respectively.

## References

1 I. Worms, D. F. Simon, C. S. Hassler and K. J. Wilkinson, *Biochimie*, 2006, **88**, 1721–1731.
2 P. G. C. Campbell, in *Metal Speciation and Bioavailability in Aquatic Systems*, ed. A. Tessier and D. R. Turner, John Wiley & Sons, Incorporated, 1995, pp. 45–102.
3 P. R. Paquin, J. W. Gorsuch, S. Apte, G. E. Batley, K. C. Bowles, P. G. C. Campbell, C. G. Delos, D. M. Di Toro, R. L. Dwyer, F. Galvez, R. W. Gensemer, G. G. Goss, C. Hogstrand, C. R. Janssen, J. C. McGeer, R. B. Naddy, R. C. Playle, R. C. Santore, U. Schneider, W. A. Stubblefield, C. M. Wood and K. B. Wu, *Comp. Biochem. Physiol., Part C: Toxicol. Pharmacol*, 2002, **133**, 3–35.
4 B. Nowack, *Environ. Sci. Technol.*, 2002, **36**, 4009–4016.
5 C. Oviedo and J. Rodriguez, *Quim. Nova*, 2003, **26**, 901–905.
6 W. G. Sunda and S. A. Huntsman, *Limnol. Oceanogr.*, 1992, **37**, 25–40.
7 W. G. Sunda and R. R. L. Guillard, *J. Mar. Res.*, 1976, **34**, 511–529.
8 J. Zeng, L. Y. Yang and W. X. Wang, *Aquat. Toxicol.*, 2009, **91**, 212–220.
9 U. S. Epa, from http://water.epa.gov/scitech/swguidance/fishshellfish/fishadvisories/technical_factsheet_2010.cfm, 2010.
10 (*a*) C. J. Watras, R. C. Back, S. Halvorsen, R. J. M. Hudson, K. A. Morrison and S. P. Wente, *Sci. Total Environ.*, 1998, **219**, 183–208; (*b*) A. F. Castoldi, T. Coccini, S. Ceccatelli and L. Manzo, *Brain Res. Bull.*, 2001, **55**, 197–203.
11 (*a*) G. C. Compeau and R. Bartha, *Appl. Environ. Microbiol.*, 1985, **50**, 498–502; (*b*) E. J. Kerin, C. C. Gilmour, E. Roden, M. T. Suzuki, J. D. Coates and R. P. Mason, *Appl. Environ. Microbiol.*, 2006, **72**, 7919–7921; (*c*) C. C. Gilmour, E. A. Henry and R. Mitchell, *Environ. Sci. Technol.*, 1992, **26**, 2281–2287.
12 (*a*) C. C. Gilmour, D. A. Elias, A. M. Kucken, S. D. Brown, A. V. Palumbo, C. W. Schadt and J. D. Wall, *Appl. Environ. Microbiol.*, 2011, **77**, 3938–3951; (*b*) J. M. Parks, A. Johs, M. Podar, R. Bridou, R. A. Hurt, S. D. Smith, S. J. Tomanicek, Y. Qian, S. D. Brown, C. C. Brandt, A. V. Palumbo, J. C. Smith, J. D. Wall, D. A. Elias and L. Y. Liang, *Science*, 2013, **339**, 1332–1335.
13 (*a*) J. M. Benoit, C. C. Gilmour and R. P. Mason, *Environ. Sci. Technol.*, 2001, **35**, 127–132; (*b*) T. Barkay, M. Gillman and R. R. Turner, *Appl. Environ. Microbiol.*, 1997, **63**, 4267–4271; (*c*) J. M. Benoit, C. C. Gilmour, R. P. Mason and A. Heyes, *Environ. Sci. Technol.*, 1999, **33**, 1780; (*d*) J. M. Benoit, R. P. Mason and C. C. Gilmour, *Environ. Toxicol. Chem.*, 1999, **18**, 2138–2141.
14 J. K. Schaefer, S. S. Rocks, W. Zheng, L. Y. Liang, B. H. Gu and F. M. M. Morel, *Proc. Natl. Acad. Sci. U. S. A.*, 2011, **108**, 8714–8719.
15 A. L. Dahl, J. Sanseverino and J. F. Gaillard, *Environ. Chem.*, 2011, **8**, 552–560.
16 T. Zhang, B. Kim, C. Leyard, B. C. Reinsch, G. V. Lowry, M. A. Deshusses and H. Hsu-Kim, *Environ. Sci. Technol.*, 2012, **46**, 6950–6958.

17 (*a*) J. K. Schaefer and F. M. M. Morel, *Nat. Geosci.*, 2009, **2**, 123–126; (*b*) U. Ndu, R. P. Mason, H. Zhang, S. J. Lin and P. T. Visscher, *Appl. Environ. Microbiol.*, 2012, **78**, 7276–7282.
18 G. R. Golding, C. A. Kelly, R. Sparling, P. C. Loewen, J. W. M. Rudd and T. Barkay, *Limnol. Oceanogr.*, 2002, **47**, 967–975.
19 B. Müller, from http://www.eawag.ch/research_e/surf/Researchgroups/sensors_and_analytic/chemeql.html, 2009.
20 P. M. May, D. Rowland and K. Murray, from http://jess.murdoch.edu.au/jess_home.htm, 2013.
21 J. Carlsson, G. P. D. Granberg, G. K. Nyberg and B. K. Edlund, *Appl. Environ. Microbiol.*, 1979, **37**, 383–390.
22 E. A. Meighen, *Microbiol. Rev*, 1991, **55**, 123–142.
23 A. Heitzer, B. Applegate, S. Kehrmeyer, H. Pinkart, O. F. Webb, T. J. Phelps, D. C. White and G. S. Sayler, *J. Microbiol. Methods*, 1998, **33**, 45–57.
24 W. Jiang, A. Saxena, B. Song, B. B. Ward, T. J. Beveridge and S. C. B. Myneni, *Langmuir*, 2004, **20**, 11433–11442.
25 B. Mishra, E. J. O'Loughlin, M. I. Boyanov and K. M. Kemner, *Environ. Sci. Technol.*, 2011, **45**, 9597–9603.
26 (*a*) U. Skyllberg, P. R. Bloom, J. Qian, C. M. Lin and W. F. Bleam, *Environ. Sci. Technol.*, 2006, **40**, 4174–4180; (*b*) K. Xia, U. L. Skyllberg, W. F. Bleam, P. R. Bloom, E. A. Nater and P. A. Helmke, *Environ. Sci. Technol.*, 1999, **33**, 257–261; (*c*) D. Hesterberg, J. W. Chou, K. J. Hutchison and D. E. Sayers, *Environ. Sci. Technol.*, 2001, **35**, 2741–2745.
27 T. Barkay, S. M. Miller and A. O. Summers, *FEMS Microbiol. Rev.*, 2003, **27**, 355–384.
28 Z. Ma, F. E. Jacobsen and D. P. Giedroc, *Chem. Rev.*, 2009, **109**, 4644–4681.
29 (*a*) B. J. Fuhr and D. L. Rabenstein, *J. Am. Chem. Soc.*, 1973, **95**, 6944–6950; (*b*) B. V. Cheesman, A. P. Arnold and D. L. Rabenstein, *J. Am. Chem. Soc.*, 1988, **110**, 6359–6364.
30 T. J. Beveridge, *J. Bacteriol.*, 1999, **181**, 4725–4733.
31 G. Berthon, *Pure Appl. Chem.*, 1995, **67**, 1117–1240.

 